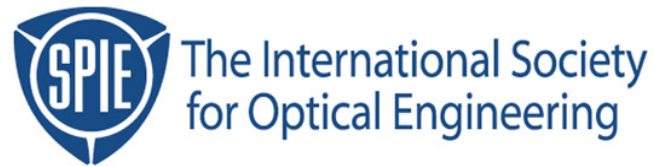


Copyright 2001 by the Society of Photo-Optical Instrumentation Engineers.



This paper was published in the proceedings of
Advances in Resist Technology and Processing XVIII,
SPIE Vol. 4345, pp. 1022-1036.

It is made available as an electronic reprint with permission of SPIE.

One print or electronic copy may be made for personal use only. Systematic or multiple reproduction, distribution to multiple locations via electronic or other means, duplication of any material in this paper for a fee or for commercial purposes, or modification of the content of the paper are prohibited.

Examination of a simplified reaction-diffusion model for post exposure bake of chemically amplified resists

Mark D. Smith*, Chris A. Mack*
KLA-Tencor Corp.

ABSTRACT

For a chemically amplified resist (CAR), the simulation of the post exposure bake (PEB) process is computationally very expensive when compared with simulation of PEB for a conventional resist. The reason for the additional computational difficulty for a CAR is that the commonly accepted mechanism for acid-catalyzed deprotection of the polymer resin requires the acid to diffuse and react simultaneously. One approach to a more efficient simulation of PEB for a CAR is to decouple the reaction-diffusion model into a diffusion step followed by a reaction step. Although the decoupled model is computationally more efficient, a significant concern with the decoupled approach is its accuracy compared with the original (coupled) reaction-diffusion PEB model. In this study, the reaction-diffusion model of the PEB process for a CAR is solved analytically for the case where the diffusivity of acid is constant and no base quencher is present in the resist formulation. This special case for PEB of a CAR allows a systematic investigation of the differences between coupled and decoupled reaction-diffusion models. It is shown that the dynamics of the PEB process predicted by the coupled reaction-diffusion model cannot be reproduced by a decoupled model. Specifically, the two models cannot be matched to predict the same dynamics for both short-time responses, such as the damping of standing wave corrugations in the resist profile, and long-time responses, such as the resist contribution to iso-dense bias or line-end shortening.

Keywords: post exposure bake, chemically amplified resists, lithography simulation, PROLITH

1. INTRODUCTION

As feature sizes continue to shrink, the ability to accurately predict critical dimensions during the patterning process becomes more important, and errors that were once perceived as insignificant now can consume much of the error budget of a tightly-controlled process. While this may seem obvious when referring to leading-edge manufacturing processes, the same is also true for simulation of these processes. If lithography simulation is used to develop and design new lithography processes, the predictions of the simulation must faithfully represent the process under consideration, and with smaller feature sizes and tighter error budgets, the accuracy of a numerical simulation becomes more important.

However, more accurate simulations of complicated processes often require greatly increased computational resources. Simulation of post-exposure bake (PEB) for a chemically amplified resist (CAR) can be especially time-consuming because the commonly-accepted mechanism for the deblocking of the polymer resin requires that the photoacid diffuse and react simultaneously. One approach to reduce the computational cost of PEB simulations is to decouple the reaction and the diffusion kinetics. However, while this approach requires much less computer time, the accuracy of such an approximation has not been previously investigated with sufficient thoroughness.

* mark.d.smith@kla-tencor.com, phone 1-512-381-2318; 8834 North Capital of Texas Highway, Suite 301, Austin, TX 78759

In this paper, we systematically study the error due to decoupling the reaction and diffusion steps. The outline of our approach is as follows. In Section 2, we outline the set of reaction-diffusion equations used to model PEB for a CAR. In Section 3, we find the exact solution to the set of reaction-diffusion equations for the case when the diffusivity is constant and no base quencher is present. Then, in Section 4, we construct approximate solutions by decoupling the reaction and diffusion steps. Approximate, decoupled solutions are constructed which match diffusion and reaction of standing waves (short-time behavior) and which match diffusion and reaction of the image in the plane of the resist (long-time behavior). In Section 5, we use PROLITH to simulate the decay of standing wave corrugations, iso-dense bias, and line-end shortening to evaluate the accuracy of the approximate models as compared with the fully coupled reaction-diffusion model of PEB. Finally, in Section 6, we summarize our results and offer our conclusions.

2. GOVERNING EQUATIONS

For a CAR, the simulation of PEB consists of two steps [1]. First, room temperature diffusion occurs when the acid generated during exposure diffuses through the resist. This can be described by the simple diffusion equation (shown here in two dimensions)

$$\frac{\partial H}{\partial t} = D(T_{amb}) \left[\frac{\partial^2 H}{\partial x^2} + \frac{\partial^2 H}{\partial z^2} \right] \quad (1)$$

where $H(x, z, t)$ is the concentration of acid, D is the diffusivity, and T_{amb} is the ambient temperature. For the analysis here, the diffusivity D is assumed to be only a function of temperature. The second step in the simulation of the PEB process is the actual bake, which is modeled as a reaction-diffusion system,

$$\frac{\partial H}{\partial t} = D(T_{PEB}) \left[\frac{\partial^2 H}{\partial x^2} + \frac{\partial^2 H}{\partial z^2} \right] - k_{loss}H - k_{quench}HB \quad (2)$$

$$\frac{\partial P}{\partial t} = -k_{amp}HP \quad (3)$$

$$\frac{\partial B}{\partial t} = -k_{quench}HB \quad (4)$$

where $P(x, z, t)$ is the concentration of blocked polymer sites, $B(x, z, t)$ is the concentration of base quencher, k_{loss} is the rate constant for the acid loss reaction, k_{quench} is the rate constant for the acid-base quenching reaction, and k_{amp} is the rate constant for the acid-catalyzed deblocking reaction. During the bake step, it is more realistic to allow the diffusivity D to be a function of P , but that case will not be considered here. Other reaction orders in Eq. (3) are possible, but only first order will be used in this analysis.

The boundary conditions for the room-temperature diffusion step and the bake step are usually chosen to be no flux at the boundaries,

$$\frac{\partial H}{\partial x} = 0, \quad x = 0, L_x \quad (5)$$

$$\frac{\partial H}{\partial z} = 0, \quad z = 0, L_z \quad (6)$$

where L_x and L_z are the pitch and the thickness of the resist, respectively. The initial condition for the concentration of acid is given by the latent image generated by exposure. The latent image from exposure is assumed to be an arbitrary function $g(x, z)$. For the room-temperature diffusion step, the initial condition is simply

$$H(x, z, 0) = g(x, z) \quad (7)$$

The concentration of acid at the end of the room-temperature diffusion step is used as the initial condition for the bake step.

3. DERIVATION OF EXACT SOLUTION FOR PEB MODEL

For the case where there is no base quencher present, a solution to the initial-value problems described above can be obtained by assuming that the solution can be written as a Fourier series. The solution for the concentration of photoacid after the room-temperature diffusion step of duration t_{RT} is given by

$$H(x, z, t_{RT}) = \sum_{i \geq 0, j \geq 0} g_{ij} \exp \left\{ - \left[\left(\frac{\pi i}{L_x} \right)^2 + \left(\frac{\pi j}{L_z} \right)^2 \right] \frac{\sigma_{RT}^2}{2} \right\} \cos \left(\frac{\pi i x}{L_x} \right) \cos \left(\frac{\pi j z}{L_z} \right) \quad (8)$$

where the coefficients g_{ij} are the coefficients of a double-cosine transformation of the initial condition $g(x, z)$, e.g.,

$$g(x, z) = \sum_{i \geq 0, j \geq 0} g_{ij} \cos \left(\frac{\pi i x}{L_x} \right) \cos \left(\frac{\pi j z}{L_z} \right) \quad (9)$$

and the room-temperature diffusion length is defined as

$$\sigma_{RT} \equiv \sqrt{2D(T_{amb})t_{RT}} \quad (10)$$

The concentration of photoacid given by Eq. (8) is used as an initial condition for the bake step. The complete solution for the concentration of acid during the bake step has a form very similar to the solution for the room temperature diffusion step,

$$H(x, z, t) = \sum_{i \geq 0, j \geq 0} G_{ij}(\sigma_{RT}) \exp(-\gamma_{ij}\tau) \cos \left(\frac{\pi i x}{L_x} \right) \cos \left(\frac{\pi j z}{L_z} \right) \quad (11)$$

where the function $G_{ij}(\sigma_{RT})$ is defined as

$$G_{ij}(\sigma_{RT}) \equiv g_{ij} \exp \left\{ - \left[\left(\frac{\pi i}{L_x} \right)^2 + \left(\frac{\pi j}{L_z} \right)^2 \right] \frac{\sigma_{RT}^2}{2} \right\} \quad (12)$$

and γ_{ij} is given by

$$\gamma_{ij} \equiv D(T_{PEB}) \left[\left(\frac{\pi i}{L_x} \right)^2 + \left(\frac{\pi j}{L_z} \right)^2 \right] + k_{loss} \quad (13)$$

The notation $\tau = t - t_{RT}$ is introduced to denote time since the beginning of the bake.

Although the solution given by Eqns. (11) to (13) is rather complicated, each term has a distinct physical meaning, and it is worthwhile to examine these equations more closely. First, in the solution described by Eq. (11), the acid concentration is represented by the superposition of several cosine components, and for a sufficiently long bake, all of the cosine components decay to zero. Part of the decay is due to the room-temperature decay term G_{ij} , given by Eq. (12), and part of the decay is due to the PEB decay term $\exp(-\gamma_{ij}\tau)$, with the decay constant γ_{ij} given by Eq. (13).

Second, each cosine component decays at a different rate. As an example, consider two separate modes for the case where the pitch is equal to the resist thickness, $L_x=L_z$. A high frequency mode corresponding to $(i=0, j=20)$, such as a standing wave, will have a decay time constant γ_{ij} that is a factor of 100 larger than the decay constant for a cosine component in the plane of the resist with

a period equal to the pitch ($i=2, j=0$). The fact that some modes decay very rapidly, while other modes hardly decay at all is the original motivation for PEB of conventional resists: the standing wave corrugations disappear with little degradation of the low frequency modes in the plane of the resist that correspond to the aerial image.

For a CAR, the final concentration of blocked polymer sites is more important than the concentration of photoacid. The concentration P can be obtained by substituting Eq. (11) into the rate expression for the deblocking reaction, Eq. (3). The resulting differential equation is separable, and can be expressed as

$$\frac{dP}{P} = -k_{amp} \left\{ \sum_{i \geq 0, j \geq 0} G_{ij}(\sigma_{RT}) \exp(-\gamma_{ij}\tau) \cos\left(\frac{\pi i x}{L_x}\right) \cos\left(\frac{\pi j z}{L_z}\right) \right\} dt \quad (14)$$

Integration of both sides of the equation leads to the remaining concentration of blocked polymer sites at the end of the PEB process,

$$\ln\left(\frac{P}{P_0}\right) = -k_{amp} \left\{ \sum_{i \geq 0, j \geq 0} G_{ij}(\sigma_{RT}) \frac{1 - \exp(-\gamma_{ij}\tau_{PEB})}{\gamma_{ij}} \cos\left(\frac{\pi i x}{L_x}\right) \cos\left(\frac{\pi j z}{L_z}\right) \right\} \quad (15)$$

where τ_{PEB} is the duration of the bake step.

4. SIMPLIFIED PEB MODELS FOR CAR

The results derived in the previous section can be used to formulate simplified models for simulation of PEB with a CAR. Such an approach is useful because the exact solutions are not available for the case where the diffusivity is not constant (e.g., a function of the concentration of blocked sites P), and numerical solution of the equations describing the PEB process can be time consuming, especially when calculating solutions for three-dimensional resist profiles. Often a simplified model will require much shorter computer times, and these models can be used to perform preliminary calculations. After the interesting portions of the process window have been identified, the full model of the PEB process can be used to obtain more accurate results. The detailed analysis presented here for the simplified models for a constant-diffusion PEB should provide insight into the accuracy of these same approximations applied to the variable-diffusivity PEB simulations.

The numerical solution of the model equations for the PEB process can be tedious due to the presence of both reaction and diffusion during the bake step. Several approximations can be made to avoid solving a reaction-diffusion system. For example, the Weiss model [2] decouples the reaction-diffusion process by proposing a development rate model that depends only on the concentration of photoacid, not on the concentration of deblocked polymer sites. The Weiss development model is given by

$$R(H) = R_{\min} + \frac{1}{2} R_{\max} \tanh\left[\frac{R_s}{R_{\max}}(H - H_{\text{threshold}})\right] + \frac{1}{2} \sqrt{\rho_1^2 + \left\{ R_{\max} \tanh\left[\frac{R_s}{R_{\max}}(H - H_{\text{threshold}})\right] \right\}^2} \quad (16)$$

where R is the development rate, R_{\min} and R_{\max} are the minimum and maximum development rates, R_s is the slope of the rate curve, $H_{\text{threshold}}$ is the threshold acid concentration, and ρ_1 is the curvature near the acid threshold.

When the Weiss development model is used in practical calculations, the acid concentration is determined from the exposure step. The PEB process is then modeled by considering only diffusion of the photoacid. As for a conventional resist, the bake step serves to reduce standing waves in the resist profiles. With this approach, the kinetics of the amplification reaction are accounted for in the Weiss development rate equation.

The model for the PEB process used with the Weiss development rate equation is a simplification of the PEB model described in the previous two sections of this paper. Note that if the amplification reaction is assumed to occur during PEB *without acid diffusion or acid loss*, Eq. (3) can be solved to obtain

$$\ln\left(\frac{P}{P_0}\right) = -k_{amp} H_{RT} \tau_{PEB} \quad (17)$$

where H_{RT} is the concentration of acid after the room-temperature diffusion step, given by Eq. (8). Furthermore, with the assumption that the value of $H_{threshold}$ accounts for the average amount of acid removed due to a loss reaction or base quencher, then the term H_{RT} in Eq. (17) is replaced with the term $(H_{RT} - H_{threshold})$ and the following expression can be obtained:

$$H_{RT} - H_{threshold} = -\frac{1}{k_{amp} \tau_{PEB}} \ln\left(\frac{P}{P_0}\right) \quad (18)$$

If Eq. (18) is substituted into the Weiss development rate model, Eq. (16), then the development rate can be calculated as a function of deblocked polymer concentration, which is a more typical form for a development rate equation.

The derivation presented above demonstrates that the Weiss model is consistent with the more conventional PEB model, Eqns. (1) to (4), if one considers diffusion only during the room-temperature diffusion step and then only reaction during the bake step. Of course, there are other interpretations to the meanings of each of the parameters in the Weiss model. However, the Weiss model *is not consistent* with a model that accounts for simultaneous reaction and diffusion. This is most readily apparent by noting that while the development rate depends on the concentration of photoacid, the development rate does not depend on the concentration gradients in the photoacid. Because the diffusive flux of photoacid depends on the magnitude of the concentration gradients, and not on the concentration itself, the Weiss development rate equation cannot predict variations in the resist profiles due to diffusion of photoacid occurring simultaneously with the deblocking reaction. In other words, the diffusion of photoacid is modeled during the bake step, and then the deblocking reaction is modeled indirectly through the Weiss development rate equation. Because the primitive variable for the chemical reaction (the concentrations) and the primitive variable for diffusion (the concentration gradients) do not appear in the same process step, it is mathematically impossible to model any coupling between the reaction and diffusion processes when using the Weiss development model.

The simplified PEB models presented in the remainder of the paper are based on the same simplification inherent in the Weiss model: the reaction and diffusion processes are decoupled. The goal of the remainder of this paper is to determine if it is possible to approximate accurately the reaction-diffusion process. However, since it has been shown that the Weiss model is equivalent to a special case of the model presented in the previous two sections, it will not be considered any further.

Mathematically, a decoupled model corresponds to setting the diffusivity during the bake step to zero. This approximation leads to a blocked polymer concentration given by

$$\ln\left(\frac{P}{P_0}\right) = -k_{amp} \left\{ \sum_{i \geq 0, j \geq 0} G_{ij}(\sigma_{RT}) \frac{1 - \exp(-k_{loss} \tau_{PEB})}{k_{loss}} \cos\left(\frac{\pi i x}{L_x}\right) \cos\left(\frac{\pi j z}{L_z}\right) \right\} \quad (19)$$

If significant standing waves are present in the latent image, diffusion during the bake step will not be negligible, and the approximation given by Eq. (19) will be inaccurate. Diffusion of the photoacid during the bake step is also important for accurately predicting iso-dense bias and line-end shortening.

Another approach is to increase the room-temperature diffusion length σ_{RT} to account for the diffusion that occurs during the bake step. This approximation will be accurate if the new room-temperature diffusion length $\tilde{\sigma}_{RT}$ can be chosen such that Eqns. (15) and (19) predict the same concentration of blocked polymer sites P . This corresponds to the condition that

$$G_{ij}(\sigma_{RT}) \frac{1 - \exp(-\gamma_{ij} \tau_{PEB})}{\gamma_{ij}} = G_{ij}(\tilde{\sigma}_{RT}) \frac{1 - \exp(-k_{loss} \tau_{PEB})}{k_{loss}} \quad (20)$$

It is important to note that Eq. (20) represents a set of equations – one equation for each pair of indices (i, j) . It will not be possible to choose $\tilde{\sigma}_{RT}$ such that all of these equations are satisfied.

Physically, the reason Eq. (20) can only be satisfied for a single set of indices (i, j) is that the function G_{ij} represents the decay of a cosine component due to diffusion, whereas the function

$$R_{ij}(\tau_{PEB}) \equiv \frac{1 - \exp(-\gamma_{ij} \tau_{PEB})}{\gamma_{ij}} \quad (21)$$

represents the progression of the contribution to the deblocking reaction from the cosine component with indices (i, j) . Interchanging these two processes must be done carefully to obtain a good approximation. This is because the influence of diffusion independent of reaction on the final concentration of deblocked polymer is very different from the influence of diffusion when coupled with reaction. For example, if σ_{RT} is very large, the standing waves in the latent image could disappear prior to the bake step, i.e. $G_{SW}(\sigma_{RT} \rightarrow \infty) = 0$, where the indices on G_{ij} are chosen to represent the cosine components of the standing waves in the resist. For this case, the standing wave component of the latent acid image will make no contribution to the deblocking reaction. By contrast, long bake times combined with a smaller value of σ_{RT} will not eliminate the standing wave contribution to the deblocking reaction because $R_{SW}(\tau_{PEB} \rightarrow \infty) = 1/\gamma_{SW}$. For this case, standing waves in the latent acid image have decayed by the end of the bake, but the contribution to the deblocking reaction from the standing waves present at the beginning of the bake remains even after the latent acid image has disappeared. Later, it will be shown that the appropriate value of $\tilde{\sigma}_{RT}$ for low spatial frequencies, such as the values of (i, j) for the aerial image in the plane of the resist, will over-damp the larger spatial frequencies, such as the standing wave components. Likewise, the appropriate value of $\tilde{\sigma}_{RT}$ for the standing wave components will under-damp the components corresponding to the aerial image in the plane of the resist.

While it is not possible to construct a simplified PEB model which is equivalent to the full PEB model for a CAR, a single value of the scaling factor can be selected so that Eq. (20) is satisfied for the values of the indices (i, j) which are in some sense the “most important” in determining the dynamics of the PEB process. Insight into an appropriate choice for (i, j) in Eq. (20) can be obtained by considering the magnitude of the terms g_{ij} . Recall that the g_{ij} terms are the coefficients in the cosine transformation of the latent image in the resist after the exposure step. A typical image in resist will consist of several low frequency modes in the plane of the resist,

corresponding to nonzero g_{ij} for small values of i . The dynamics of the PEB process for these values of (i,j) will be important in correctly predicting phenomena such as iso-dense bias. In addition, there will also be nonzero values of g_{ij} for relatively large values of j – these components of the cosine transformation of the latent image represent the standing waves in the resist. Values of $\tilde{\sigma}_{RT}$ will be investigated that correctly predict the magnitude of standing waves in the resulting resist profiles and that correctly predict iso-dense bias.

4.1 Simplified PEB model for predicting the influence of standing waves

To correctly predict the influence of standing waves in the resist on the resulting resist profiles, a reasonable choice for the indices (i,j) is $i = 0$ and the value of j that best represents a standing wave pattern in the latent image from the exposure part of the simulation. The number of standing waves in the resist is approximately equal to

$$N_{sw} = \frac{2L_z}{\lambda/n} \quad (22)$$

where N_{sw} is the number of standing waves, λ is the exposure wavelength, and n is the real part of the index of refraction for the photoresist. The value of j which best represents this number of standing waves is $j = 2N_{sw}$. Substitution of this choice for (i,j) into Eq. (20) leads to an equation for the value of $\tilde{\sigma}_{RT}$ appropriate for describing standing waves, $(\tilde{\sigma}_{RT})_{sw}$:

$$\frac{1 - \exp\left(-k_{loss}\tau_{PEB} - \left(\frac{4\pi n}{\lambda}\right)^2 \frac{\sigma_{PEB}^2}{2}\right)}{k_{loss} + \left(\frac{4\pi n}{\lambda}\right)^2 \frac{\sigma_{PEB}^2}{2\tau_{PEB}}} \exp\left\{-\left(\frac{4\pi n}{\lambda}\right)^2 \frac{(\sigma_{RT})_{sw}^2}{2}\right\} = \exp\left\{-\left(\frac{4\pi n}{\lambda}\right)^2 \frac{(\tilde{\sigma}_{RT})_{sw}^2}{2}\right\} \frac{1 - \exp(-k_{loss}\tau_{PEB})}{k_{loss}} \quad (23)$$

This equation can be solved for $(\tilde{\sigma}_{RT})_{sw}$

$$(\tilde{\sigma}_{RT})_{sw} = \sqrt{\frac{2 \ln \left\{ \frac{1 - \exp\left(-k_{loss}\tau_{PEB} - \left(\frac{4\pi n}{\lambda}\right)^2 \frac{\sigma_{PEB}^2}{2}\right)}{k_{loss} + \left(\frac{4\pi n}{\lambda}\right)^2 \frac{\sigma_{PEB}^2}{2\tau_{PEB}}} \frac{k_{loss}}{1 - \exp(-k_{loss}\tau_{PEB})} \right\}}{\left(\frac{4\pi n}{\lambda}\right)^2} + \sigma_{RT}^2} \quad (24)$$

The accuracy of the results obtained by using a simplified PEB model based on Eq. (24) is examined in Section 5.

4.2 Simplified PEB model for predicting iso-dense bias

To correctly predict the contribution from the resist chemistry to iso-dense bias, the simplified PEB model must correctly account for diffusion within the plane of the resist. The set of indices (i,j) that should be chosen to calculate $\tilde{\sigma}_{RT}$ with Eq. (20) can be determined by examination of the form of the latent image in the resist from the exposure step.

At exposure, the aerial image is translated into a latent image in the plane of the resist. The chemical kinetics of the photoacid generation process can be described by

$$\frac{dG(x,t)}{dt} = -CI(x)G(x,t) \quad (25)$$

where G is the concentration of photoacid generator, C is a rate constant, and I is the intensity of the electric field in the resist. Because the goal of this derivation is to obtain estimates for the indices (i,j) , the influence of defocus within the resist will not be considered here.

For a non-bleaching, non-absorbing resist, the solution to Eq. (25) for a given dose, $I(x)t_{dose}$, is

$$\frac{G(x)}{G_0} = \exp[-CI(x)t_{dose}] \quad (26)$$

If the product $CI(x)t_{dose}$ is small for all values of x , the exponential in Eq. (26) can be expanded in a Taylor series. Furthermore, if one mole of acid is generated for each mole of photoacid generator consumed, then the concentration of acid can be written as

$$\frac{H}{G_0} = 1 - (1 - CI(x)t_{dose} + \dots) \cong CI(x)t_{dose} \quad (27)$$

As a simple example, consider the image generated from a mask with lines of width w separated by a distance L_x . The mask is described in wafer dimensions. The electric field at the focal plane for a coherent, diffraction-limited imaging system is given by

$$E(x) = \sqrt{I_0} \left\{ L_x - \sum_{n=-\infty}^{n=\infty} E_n \cos\left(\frac{2\pi nx}{L_x}\right) \right\} \quad (28)$$

where I_0 is a normalizing factor for the intensity, E_n is given by the equation

$$E_n = \begin{cases} \frac{L_x \sin\left(\frac{n\pi w}{L_x}\right)}{\pi n} & \text{for } |n| \leq N_{\max} \\ 0 & \text{for } |n| > N_{\max} \end{cases} \quad (29)$$

and N_{\max} is the maximum integer which satisfies the equation

$$N_{\max} \leq \frac{NAL_x}{\lambda} \quad (30)$$

That is, N_{\max} is the largest diffraction order that enters the pupil of the objective lens.

The intensity is the square of the electric field, so Eq. (28) can be substituted into Eq. (27) to give

$$\frac{H(x)}{G_0} = Ct_{dose}I_0 \left\{ L_x - \sum_{n=-N_{\max}}^{n=N_{\max}} E_n \cos\left(\frac{2\pi nx}{L_x}\right) \right\}^2 \quad (31)$$

Expanding the square of the electric field yields

$$\begin{aligned} \frac{H(x)}{G_0} = Ct_{dose}I_0 \left\{ (L_x - E_0)^2 + 4(L_x - E_0) \sum_{n=1}^{N_{max}} E_n \cos\left(\frac{2\pi nx}{L_x}\right) \right. \\ \left. + 4 \sum_{n=1}^{N_{max}} E_n \cos\left(\frac{2\pi nx}{L_x}\right) \left[\sum_{m=1}^{N_{max}} E_m \cos\left(\frac{2\pi mx}{L_x}\right) \right] \right\} \end{aligned} \quad (32)$$

Trigonometric identities can be used to eliminate the products of cosines and reduce Eq. (32) to a cosine series,

$$\begin{aligned} \frac{H(x)}{G_0} = Ct_{dose}I_0 \left\{ (L_x - E_0)^2 + 4(L_x - E_0) \sum_{n=1}^{N_{max}} E_n \cos\left(\frac{2\pi nx}{L_x}\right) \right. \\ \left. + 2 \sum_{n=1}^{N_{max}} \sum_{m=1}^{N_{max}} E_n E_m \left[\cos\left(\frac{2\pi(n-m)x}{L_x}\right) + \cos\left(\frac{2\pi(n+m)x}{L_x}\right) \right] \right\} \end{aligned} \quad (33)$$

Eq. (33) will be used to determine the appropriate matching conditions for the simplified PEB model that will accurately represent iso-dense bias. Because the intensity is the square of the electric field, the maximum spatial frequency in the intensity is double the maximum spatial frequency of the electric field. The maximum spatial frequency in the electric field given by Eq. (28) occurs when $n=N_{max}$, whereas the maximum spatial frequency in the intensity given by Eq. (33) occurs when $n+m=2N_{max}$. However, the largest spatial frequency may not be the most important term in the cosine expansion given by Eq. (33). Of the three terms in braces in Eq. (33), both the second term (the single summation) and the third term (the double summation) make a contribution to the spatial frequency $f_x=N_{max}/L_x$. On the other hand, only the third term (the double summation) makes a contribution to the spatial frequency $f_x=2N_{max}/L_x$. Thus, while $f_x=2N_{max}/L_x$ will be the largest spatial frequency present, the coefficient for the spatial frequency $f_x=N_{max}/L_x$ should be larger in magnitude. For this reason, the matching condition where $f_x=N_{max}/L_x$ is used, and the index i is chosen to satisfy the equation

$$\frac{\pi i}{L_x} = \frac{2\pi N_{max}}{L_x} = \frac{2\pi NA}{\lambda} \quad (34)$$

This leads to the matching condition for $\tilde{\sigma}_{RT}$ appropriate for the aerial image, given by

$$\begin{aligned} \frac{1 - \exp\left(-k_{loss}\tau_{PEB} - \left(\frac{2\pi NA}{\lambda}\right)^2 \frac{\sigma_{PEB}^2}{2}\right)}{k_{loss} + \left(\frac{2\pi NA}{\lambda}\right)^2 \frac{\sigma_{PEB}^2}{2\tau_{PEB}}} \exp\left\{-\left(\frac{2\pi NA}{\lambda}\right)^2 \frac{\sigma_{RT}^2}{2}\right\} = \\ \exp\left\{-\left(\frac{2\pi NA}{\lambda}\right)^2 \frac{(\tilde{\sigma}_{RT})_{AI}^2}{2}\right\} \frac{1 - \exp(-k_{loss}\tau_{PEB})}{k_{loss}} \end{aligned} \quad (35)$$

Finally, Eq. (35) can be solved for $(\tilde{\sigma}_{RT})_{AI}$

$$(\tilde{\sigma}_{RT})_{AI} = \sqrt{\frac{2 \ln \left\{ \frac{1 - \exp \left(-k_{loss} \tau_{PEB} - \left(\frac{2\pi NA}{\lambda} \right)^2 \frac{\sigma_{PEB}^2}{2} \right)}{k_{loss} + \left(\frac{2\pi NA}{\lambda} \right)^2 \frac{\sigma_{PEB}^2}{2\tau_{PEB}}} \frac{k_{loss}}{1 - \exp(-k_{loss} \tau_{PEB})} \right\}}{-\left(\frac{2\pi NA}{\lambda} \right)^2} + \sigma_{RT}^2} \quad (36)$$

5. DISCUSSION

The accuracy of the approximate PEB models will be examined by calculating the magnitude of standing waves in resist profiles and by calculating the iso-dense bias with both the full model and the simplified models described by Eqns. (24) and (36). Furthermore, the cost of calculating three-dimensional resist profiles will be examined. The cost of the calculation will be measured by the CPU time required to simulate the PEB process by using PROLITH Version 7.0 on a 750 MHz Pentium III workstation. All of the calculations are performed with the User-Defined CA Resist set of resist model parameters¹. Important parameters in this model include the bulk acid loss rate constant $k_{loss} = 9.97e-3 \text{ sec.}^{-1}$, the rate constant for the amplification reaction $k_{amp} = 0.15 \text{ sec.}^{-1}$, and the room temperature diffusion length $\sigma_{RT} = 20 \text{ nm}$. For this simple model, there is no base quencher in the resist formulation and no base contamination at the surface of the resist. The imaging system was chosen with $NA = 0.5$, $\lambda = 248 \text{ nm}$, and a partial coherence of 0.5.

In the first set of calculations, the magnitude of the standing waves in the resist profiles is examined. The amplitude of the standing waves is measured by fitting a straight line to the shape of the resist sidewall, and then the root-mean-square (RMS) deviation of the resist sidewall from the straight line is reported for each calculation. The bottom 20% and top 20% of the resist profile are not used in the calculation of either the straight line or the RMS deviation to avoid the influence of footing or resist loss on the reported RMS deviation from a straight sidewall shape. The diffusivity during the bake step is $D = 8.51 \text{ nm}^2/\text{sec}$. This relatively small value is chosen so that standing waves would be present in the resist profiles for a large range of bake times. The exposure dose is decreased as the thermal dose (bake time) is increased to vary σ_{PEB} while keeping the extent of the amplification reaction approximately fixed, as shown in Table 1.

The RMS deviation of the resist sidewall from a straight line is shown for several bake times and several bake models in Figure 1. As shown in the figure, the agreement between the simplified model based on Eq. (24) and the full PEB model is quite good. This indicates that the matching condition for the decay of the standing waves in resist has been chosen correctly. Also shown in Figure 1 are results for the model with no added diffusion (σ_{RT} remains at 20 nm), as described by Eq. (19). The exposure doses listed in Table 1 have been chosen so that the magnitude of the standing wave in the resist profile is almost constant for this model over the full range of bake times shown in the Figure 1. Thus, the results for the model with no added diffusion demonstrate that the magnitude of the standing wave in the resist profile is sensitive to the details of the diffusion model during the bake step.

¹ The procedure for performing decoupled calculations with PROLITH by changing model parameters is outlined in the appendix.

Exposure Dose (mJ/cm ²)	Bake Time (sec)	σ_{PEB} (nm)	$(\tilde{\sigma}_{RT})_{SW}$ (nm)	$(\tilde{\sigma}_{RT})_{AI}$ (nm)
30.21	15	15.98	22.70	22.92
14.87	30	22.60	24.55	25.36
10.35	45	27.68	25.82	27.46
8.21	60	31.96	26.84	29.30
6.97	75	35.73	27.54	30.93
6.17	90	39.14	27.98	32.36

Table 1: Exposure and bake parameters for the set of calculations investigating the magnitude of standing wave amplitude in the resist profiles. The modified room-temperature diffusion lengths, $(\tilde{\sigma}_{RT})_{SW}$ and $(\tilde{\sigma}_{RT})_{AI}$, are calculated using Eqns. (24) and (36), respectively.

The data presented in Figure 1 also demonstrate that the simplified model based on matching the diffusion of the latent image in the plane of the resist, as described by Eq. (36), is not as accurate as the model explicitly designed to match the decay of the standing waves. As expected, the standing waves in the resist profiles are over-damped. However, both of the simplified models developed in the previous section are more accurate than entirely neglecting diffusion during the bake step.

In the second set of calculations, the iso-dense bias is calculated for all four PEB models. Results are shown in Figure 2. For this set of calculations, more typical values are chosen for the diffusivity during the bake step ($D = 69.5 \text{ nm}^2/\text{sec}$) and bake time (60 seconds). The exposure dose is chosen as 8.83 mJ/cm^2 in order to size the dense lines. With this set of model parameters, $\sigma_{PEB} = 91.3 \text{ nm}$, and Eqns. (24) and (36) yield $(\tilde{\sigma}_{RT})_{SW} = 34.8 \text{ nm}$ and $(\tilde{\sigma}_{RT})_{AI} = 62.7 \text{ nm}$, respectively.

As shown in the figure, the agreement between the full PEB model and the model designed to match the diffusion of the aerial image in the plane of the resist is very good over the full range of pitches, whereas the models without additional room-temperature diffusion, described by Eq. (19), and the model matched to the diffusion of the standing waves in the resist, described by Eq. (24), do not agree well with the full PEB model. Again, this result is expected, because the matching condition for the large spatial wavenumber of the standing wave leads to smaller amount of room-temperature diffusion, and thus the resist contribution to the iso-dense bias is under-estimated.

Another interesting result is that while the value of $\tilde{\sigma}_{RT}$ for matching standing waves is very different from the value for matching the aerial image, the values of $(\tilde{\sigma}_{RT})_{AI}$ given by Eq. (36) for two different values of NA are very similar. As an example, recall that $(\tilde{\sigma}_{RT})_{AI} = 62.7 \text{ nm}$ for the imaging tool in the current study. The matching value changes to $(\tilde{\sigma}_{RT})_{AI} = 61.0 \text{ nm}$ when the NA is increased to 0.7. This implies that the same decoupled model could be used to explore the influence of stepper settings on iso-dense bias with little additional error. Indeed, if the calculation shown in Figure 2 is repeated with an imaging tool with NA=0.7, but with the value of $(\tilde{\sigma}_{RT})_{AI}$ for NA=0.5, the largest difference between the full model and the decoupled model is only about 2 nm, which is acceptable for most investigations.

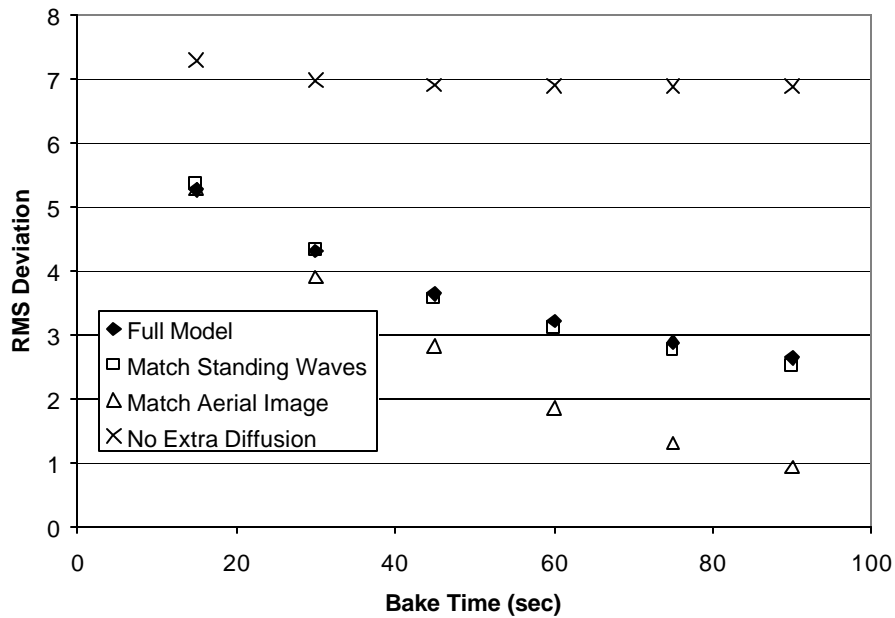


Figure 1: RMS deviation of the resist sidewalls from a straight line as calculated with the full PEB model, the simplified PEB model based on matching diffusion of standing waves, the simplified PEB model based on matching diffusion of the aerial image, and the PEB model with no diffusion during the bake step.

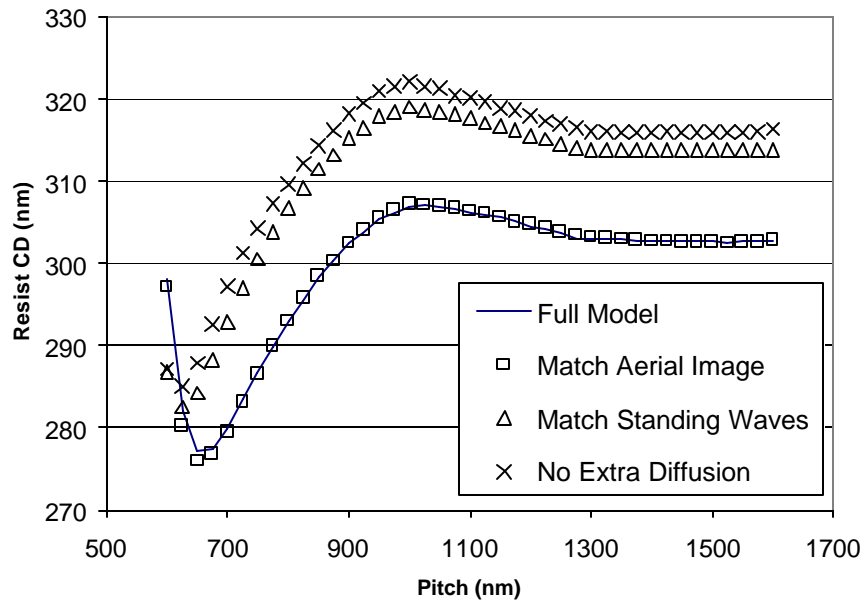


Figure 2: Iso-dense bias for 300 nm lines as a function of pitch for the full PEB model, the simplified model for matching the standing waves, the simplified model for matching the aerial image, and the simplified model with no additional diffusion.

	Pull-back (nm)	CPU Time (sec)
Full Model	45.6	30.8
Match Standing Waves	39.1	3.4
Match Aerial Image	44.8	3.3
No Extra Diffusion	41.5	3.3

Table 2: Calculated pull-back and CPU times for a 250 nm line-end shortening simulation for all four PEB models.

For the last set of calculations, the accuracy and cost of simulation of the PEB process for a three-dimensional resist profile will be examined. Here line-end-shortening for 250nm lines separated by a 250 nm gap is examined. The model parameters for this calculation are the same as used for the iso-dense bias study, except that the exposure dose has been slightly increased to 9.0 mJ/cm². The calculated pull-back of the line end for each of the models is given in Table 2. The simplified model based on matching the diffusion of the aerial image within the plane of the resist calculates a value of the pull-back that is within 0.8 nm of the value calculated with the full model. Furthermore, the CPU time required for the simplified model is almost a factor of ten smaller than the CPU time required for a calculation with the full PEB model. The simplified models with no added diffusion or with extra diffusion to match the contribution of the standing waves are less accurate. This is further demonstrated in Figure 3, where the cross-section of the line end is shown for all four models. All three of the simplified models behave as expected for a more complicated, three-dimensional resist pattern. First, the model based on matching the standing waves fails to accurately calculate the amount of pull-back for the line end, but this model does accurately predict the magnitude of the standing waves on the resist sidewall. The second model shown in Figure 3, which is designed to match the diffusion of the aerial image with the plane of the resist, does an excellent job of predicting the amount of pull-back. Although the amplitude of the standing waves is incorrect, the overall shape of the resist profile is in good agreement with the resist profile calculated by using the full PEB model. Finally, the simplified model with no additional diffusion predicts neither the overall shape nor the amplitude of the standing waves correctly. As was found in all of the calculations in this section, this model cannot predict even qualitatively correct resist profiles, and these results demonstrate that additional room-temperature diffusion is necessary to obtain reasonable results.

6. SUMMARY AND CONCLUSIONS

In this study, a Fourier series was used to obtain an exact solution for a PEB model for chemically amplified resists. This exact solution was used to develop simplified PEB models and to determine the accuracy of these models. Specifically, the examination included simplified models that decouple the reaction-diffusion equation. This equation describes the diffusion of photoacid and the deblocking of the polymer resin during the bake process. The most important result of this study is that, if the PEB process is split into a diffusion step followed by a reaction step, it is only possible to match the magnitude of a single Fourier component in the simplified model with the solution for the full PEB model. The latent image in resist after exposure will typically contain many spatial frequencies, so no combination of model parameters in a decoupled model can lead to a deblocked polymer concentration at the end of the PEB process that is consistent with the concentrations calculated with the full PEB model.

Nevertheless, reasonably accurate resist profiles can be obtained by matching the Fourier component that is the “most important” part of the latent image in the resist. Two matching

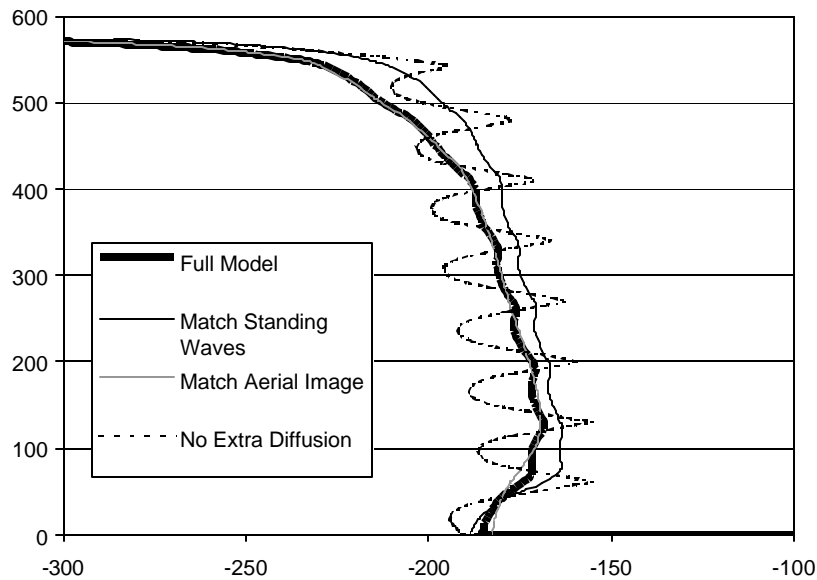


Figure 3: Cross-section of the line end as calculated with the full PEB model, the simplified PEB model for matching the standing waves, the simplified model for matching the aerial image, and the simplified model with no added diffusion.

conditions that are useful for determining parameter values for decoupled PEB models have been examined. The first matching condition ensures that the magnitude of the standing waves in the resist profile is accurately predicted by the decoupled PEB model. However, the decoupled PEB model based on this matching condition does not accurately predict effects related to the diffusion of the photoacid within the plane of the resist. Specifically, both iso-dense bias and line-end shortening are underestimated. A second matching condition is proposed which ensures that the diffusion of the latent image in the plane of the resist is accurately predicted by the simplified models. Although this model accurately predicts iso-dense bias and line-end shortening, the standing waves in the resist profiles are over-damped. As demonstrated in the line-end shortening results presented in Figure 3, the simplified models that decouple the reaction from the diffusion can accurately predict either the dimensions of the resist profiles or the magnitude of the standing waves, but not both of these features at the same time.

However, a significant drawback of the matching approach used in this study is that the parameters in the PEB model depend on the imaging tool – to match the standing waves in the resist, one must know the exposure wavelength, and to match diffusion within the plane of the resist, one must know the numerical aperture of the lens. This artificial coupling between the exposure model and the bake model parameters underscores the fact that a bake model that decouples reaction and diffusion cannot reproduce the results from a coupled reaction-diffusion model of the PEB process. Because the reaction-diffusion model is so widely accepted within the field of photolithography, the simplified, decoupled PEB models should be used only for preliminary calculations, and all simulations that require any degree of accuracy should be performed with a fully-coupled reaction-diffusion model of the PEB process.

7. ACKNOWLEDGEMENTS

The authors would like to thank Jeff Byers for many helpful discussions.

8. REFERENCES

1. C.A. Mack, *Inside PROLITH: A Comprehensive Guide to Optical Lithography Simulation*, FINLE Technologies, (Austin, TX: 1997).
2. M. Weiss, H. Binder, R. Schwalm, “Modeling and simulation of a chemically amplified DUV resist using the effective acid concept,” *Microelectronic Engineering*, Vol. 27 (1995) pp. 405-408.
3. J. Byers, J. Petersen, and J. Sturtevant, “Calibration of Chemically Amplified Resist Models,” *Advances in Resist Technology and Processing XIII, Proc.*, SPIE Vol. 2724 (1996) pp. 156-162.
4. J. Petersen and J. Byers, “Examination of Isolated and Grouped Feature Bias in Positive Acting, Chemically Amplified Resist Systems,” *Advances in Resist Technology and Processing XIII, Proc.*, SPIE Vol. 2724 (1996) pp. 163-171.
5. P.W. Atkins, *Physical Chemistry*, 4th edition, Oxford University Press (New York, NY: 1990)

8. APPENDIX: KINETICS FOR THE DEBLOCKING REACTION IN PROLITH

In the current study, the model parameters in PROLITH are manipulated to compare coupled and decoupled models for PEB. Decoupled calculations are performed by setting the room temperature diffusion length to the value of $\tilde{\sigma}_{RT}$ given by Eqns. (24) or (36), and then setting the value of D for the resist to be very small. However, a good choice for the value of the diffusivity is more complicated than it may initially seem due to the inclusion of a sophisticated kinetic model of the deblocking reaction. We outline the kinetic model below, and then we explain how the diffusivity should be chosen in PROLITH to simulate decoupled PEB models.

The kinetic model for the deblocking reaction proposed by Byers, Petersen, and Sturtevant [3], and Petersen and Byers [4] has been adopted in PROLITH v6.0 and v7.0. This reaction model is a superset of the reaction kinetics given by Eq. (3). In the newer model, the amplification reaction is thought to occur by two sequential steps. First, acid diffuses to the reaction site and forms an intermediate group where the acid is close enough to the blocked polymer site to catalyze the deblocking reaction. In the second step of the deblocking reaction, the acid reacts at the blocked polymer site and deblocks the polymer. The overall reaction rate is described by the equation

$$K_{overall} = \frac{K_a K_{diff} D}{K_a + K_{diff} D} \quad (37)$$

where K_{diff} is the diffusion-controlled reaction constant and K_a describes the rate of the reaction when the acid and blocking group are in close proximity. The overall rate of the deblocking reaction given by Eq. (37) then replaces the value of K_{amp} in Eq. (3). As demonstrated by the equation, the value of $K_{overall}$ is a balance between the rate at which the acid can move to a blocked polymer site (described by the product $K_{diff} D$) and the rate at which the acid reacts after it has reached the polymer site (described by K_a). Further information regarding this model, including a derivation of Eq. (37), can be found in most physical chemistry texts (e.g., [5]).

The “very small” value of the diffusivity chosen when performing decoupled calculations must be chosen carefully, because the value of $K_{overall}$ as given by Eq. (37) depends on the value of D . However, for the purpose of the comparison in the current study, the value of $K_{overall}$ should be the same for the coupled and the decoupled models. This problem was circumvented by setting K_{diff} to be very large, typically 10^5 nm^{-2} , and then choosing D to be “very small”, but not too small: we used a value of $10^{-3} \text{ nm}^2/\text{sec}$. When $K_{diff} D \gg K_a$, the value of $K_{overall}$ will be independent of D and equal to K_a , which is set to $K_a=0.15 \text{ sec}^{-1}$ for both the coupled and the decoupled models.